Theory of core-hole effects in 1*s* core-level spectroscopy of the first-row elements

Shang-Peng Gao,[1] Chris J. Pickard,[2] Mike C. Payne,[1] Jing Zhu,[3] and Jun Yuan[3]
[1]*Theory of Condensed Matter, Cavendish Laboratory, J. J. Thomson Avenue, Cambridge CB3 0HE, United Kingdom*
[2]*School of Physics and Astronomy, University of St Andrews, St Andrews KY16 9SS, United Kingdom*
[3]*Department of Materials Science and Engineering, Tsinghua University, Beijing 100084, Peoples' Republic of China*
(Received 30 May 2007; revised manuscript received 20 December 2007; published 18 March 2008)

The 1*s* core-level excited spectra in LiF, BeO, cubic BN, CaB_6, MgB_2, SiC, diamond, and C_3N_4 were calculated using an *ab initio* pseudopotential plane wave method and a projector augmented wave reconstruction. Core-hole effects were investigated through a detailed examination of spectral differences between theoretical results from standard ground state calculations and from supercell calculations that included the core hole. A quantitative analysis reveals a relationship between core-hole strength and the valence charge population.

DOI: 10.1103/PhysRevB.77.115122 PACS number(s): 71.20.−b, 79.20.Uv, 61.05.cj, 71.15.−m

I. INTRODUCTION

Through electron or x-ray spectroscopy, probing the excitations of electrons from core levels to unoccupied electronic states is a basic tool for investigating the properties of materials. Electron energy-loss near-edge structure (ELNES) and x-ray absorption near-edge structure (XANES) probe information on the unoccupied electronic states by exciting one electron from a core level into the unoccupied states. (Scanning) transmission electron microscopes with an electron energy-loss spectrometer attached have been used extensively in the study of nanoscale materials to obtain information about local composition, structure, and electronic structure. However, the probing electron (or x-ray) actually interacts with a system that has been perturbed by the probe itself, with an inner-shell electron removed, i.e., with a core hole.[1–4] The relaxation of the system in the presence of the core hole will affect the observed core-level excitation spectra so that interpretation of the experimental spectrum becomes a more challenging task. A satisfactory theory of optical spectra or core excited spectra should calculate two-particle electron-hole interactions in a reliable and accessible way. In the core-level excitation process, the core hole is localized on a single atomic site. Using an atom with a reduced occupation in the core level within a supercell approximation has been a good and popular description for the calculation of core-level spectroscopy within standard density functional theory (DFT).[4–12] Recent developments on core-level spectroscopy calculation using the Bethe-Salpeter equation[13,14] or time-dependent DFT[15] or a combination of the two approaches[16,17] provide more rigorous approaches for a core-level spectra calculation. In these approaches, many-body effects such as the broadening of spectra due to electron-hole lifetime can be taken into account in a natural way. While good agreement with experimental results has been achieved, this necessarily comes with a much greater computational burden as compared to standard ground state calculations.

A systematic observation of core-hole effects and a quantitative estimation of the core-hole strength in materials can assist in the simulation and interpretation of core-level spectra. If based on some empirical rules, we can predict that a certain core-level spectrum is not likely to be heavily influenced by core-hole effects, information on the ground electronic structure of a material can be inferred directly from the experimental spectrum. In this case, traditional ground state calculations will be expected to predict the main features of experimental results and so allow interpretation of the experimental spectrum. If this is not the case, inclusion of the influence of the core hole is essential in the theoretical simulation, and one should be aware in the analysis of experimental results that near-edge fine structure includes influences in the core excitation process beyond the ground state electronic structure.

Core-hole effects have been observed in many spectra by numerous authors.[8,10,12–14,18–24] The conductivity and dielectric constant[4,20] have been suggested as important factors related to the core-hole influence due to their connection with electron screening. In the study of core excitons of alkali halides[1,21] through the comparison of ground state calculation results with x-ray absorption spectra, it is found that the exciton is more strongly bound at the cation than at the anion site. This finding is explained by the difference in the effective screening of valence electrons.[1]

Given the wide scope of the materials studied by core-level spectroscopy, a systematic investigation of core-hole influence is desirable to determine the factors correlated with core-hole strength. In the present paper, core-hole effects in a series of materials consisting of seven first row elements (excluding neon) have been studied by comparing standard ground state calculations with calculations that include core-hole correction. We chose first row elements as the primary system for the study of core-hole effects because of their simplicity for a theoretical investigation and their importance in the application of core-level spectroscopy. During the excitation process in the first row elements, only the *K* edges are formed and the screening effect of the remaining core electron (i.e., the other 1*s* electron) is similar. This brings the simplicity of isolating the effect of valence electrons from that of core electrons. To fully take account of the latter for all possible excitations would involve careful classification and discussion of the atomiclike core orbitals and their different possible initial states (*K*, L_1, $L_{2,3}$, etc.). From the viewpoint of experimental application, the *K* edges of light elements B, C, N, and O are ideal for the electron energy-loss

TABLE I. Lattice parameters and supercell size in spectra simulations including the core-hole effects.

	Space group	Lattice constant (Å)	Supercell size
LiF	$Fm\bar{3}m$ (225)	a=4.027	3×3×3 (54 atoms)
BeO	$P6_3mc$ (186)	a=2.696, c=4.379, u=0.3771	3×3×2 (72 atoms)
c-BN	$F\bar{4}3m$ (216)	a=3.6162	3×3×3 (54 atoms)
Diamond	$Fd\bar{3}m$ (227)	a=3.567	3×3×3 (54 atoms)
CaB_6	$Pm\bar{3}m$ (221)	a=4.146	2×2×2 (56 atoms)
MgB_2	$P6/mmm$ (191)	a=3.0864, c=3.5215	3×3×2 (56 atoms)
β-SiC	$F\bar{4}3m$ (216)	a=4.358	3×3×3 (54 atoms)
β-C_3N_4	$P3$ (143)	a=6.4017, c=2.4041	1×1×3 (42 atoms)

spectroscopy study because of both the large cross section and the detailed fine structures that reflect local structure and bonding environments.[25–28] A quantitative method is introduced to estimate the strength of the core-hole effect in these K edges. A clear relationship between core-hole strength and valence charge population of the excited atom is found.

II. CALCULATION METHOD

A. Electronic structure calculation

Our calculations are based on a plane wave pseudopotential method within the framework of density functional theory,[29–31] which has the advantage of being computationally less intensive than an all-electron code, such as OLCAO (Ref. 5) or FPLAPW.[11] Pseudopotential codes have been used in the past for ELNES/XANES calculations, but often without fully taking into account the matrix element effect and ignoring the pseudopotential error in the core region, thus failing to give an absolute value of matrix elements and thus an absolute cross section value. In our approach, matrix elements are explicitly calculated and the pseudopotential error is eliminated through a reconstruction of all electron calculation results after the band structure calculation (see Sec. II B below). In this way, both the advantage of the pseudopotential method, i.e., reduced computational cost and the ability to do very large systems, and the accuracy of all-electron methods are retained.

The interaction between the core hole and the excited electron was treated within the single-particle electronic structure method[4,8–10,35] by taking the advantage of the localization of the core hole. To model the excited atom in which the hole is localized, a pseudopotential for the excited state was specially constructed by reducing the occupation of the core level of the reference configuration by 1. A supercell approximation is adopted to minimize the mutual interaction of excited centers. The lattice parameters of the materials studied and the supercell sizes for the calculations that include core-hole effects are shown in Table I. For the theoretically proposed material β-C_3N_4,[36] the equilibrium structural parameters calculated by Teter and Hemley[37] were employed. The minimum core-hole to core-hole distances for each structure corresponding to the parameters given in Table I are 8.54 Å for LiF, 8.09 Å for BeO, 7.67 Å for c-BN, 7.57 Å for diamond, 8.29 Å for CaB_6, 7.04 Å for MgB_2, 9.24 Å for β-SiC, and 6.40 Å for β-C_3N_4.

The choice of supercells in Table I is a compromise between computational burden and accuracy. All the calculations can be performed using a PC (2.8 GHz Pentium 4 together with 2 Gbytes random access memory). The confidence on the reliability of the calculated results using the chosen supercell size is based on the following arguments. Although the exact convergence condition of supercell size relates to a specific system, our experience[6,8,22,38,39] and test calculations using supercell size smaller than that in Table I show that a supercell size with a minimum distance between neighboring excited atoms larger than about 6 Å can generally give theoretical spectra consistent with experimental measurement. Limited tests using a larger and more computational consuming system such as a 4×4×4 (128 atoms) supercell for diamond also confirm our expectation; i.e., our choice can give fairly reliable results, sufficient for our purposes, while requiring only easily accessible computational resources. However, we also admit that for very detailed features, such as for the interpretation of the results obtained by high energy resolution data, a more stringent test for the convergence of supercell might be required.

Vanderbilt ultrasoft pseudopotentials[32] were employed, using the generalized gradient-corrected functional exchange-correlation approximation.[33] The Monkhorst-Pack scheme[34] including symmetry was applied for a Brillouin zone integration of each supercell. The number of k points sampled in the irreducible wedge is equivalent to 64 k points in the first Brillouin zone. The maximum k-point spacings are 0.225 $Å^{-1}$ for LiF, 0.224 $Å^{-1}$ for BeO, 0.251 $Å^{-1}$ for c-BN, 0.254 $Å^{-1}$ for diamond, 0.189 $Å^{-1}$ for CaB_6, 0.223 $Å^{-1}$ for MgB_2, 0.208 $Å^{-1}$ for β-SiC, and 0.283 $Å^{-1}$ for β-C_3N_4. The plane wave cutoff energy was chosen to be around 400 eV.

B. Energy-loss near-edge structure simulation

The dipole approximation is justified for most transmission electron energy-loss spectroscopy experiments, particularly when a small axial collection aperture is employed. For K-edge spectra, the p-symmetry unoccupied states are

probed.[25] The electric dipole approximation applies for x-ray absorption spectroscopy when the wavelength of the x-ray, which induces the transition, is much larger than the size of the core orbital. The key part of an ELNES/XANES calculation within the dipole approximation is the calculation of the matrix elements of the position operator between the core state $|\phi_c\rangle$ on the site of interest, which can be obtained from an all-electron atomic calculation, and the unoccupied final state $|\psi_{n,k}\rangle$. According to the projector augmented wave (PAW) approach,[40] an all-electron wave function $|\psi_{n,k}\rangle$ can be recovered from the corresponding pseudo-wave-function $|\tilde{\psi}_{n,k}\rangle$ via a linear transformation.

Following the previous work of Pickard and co-workers,[8,10,35] the dipole matrix elements are evaluated by using the PAW approach to remove errors due to the pseudopotential,

$$\langle \phi_c|r_\alpha|\psi_{n,k}\rangle = \langle \phi_c|r_\alpha|\tilde{\psi}_{n,k}\rangle + \sum_i \left(\langle \phi_c|r_\alpha|\phi_i\rangle - \langle \phi_c|r_\alpha|\tilde{\phi}_i\rangle\right) \times \langle \tilde{p}_i|\tilde{\psi}_{n,k}\rangle, \quad (1)$$

where ϕ_i and $\tilde{\phi}_i$ are all-electron and pseudopartial waves, respectively, and $\alpha = x,y,z$. $(\langle \phi_c|r_\alpha|\phi_i\rangle - \langle \phi_c|r_\alpha|\tilde{\phi}_i\rangle)$ can be evaluated once in real space for each pseudopotential used. $\tilde{p}_i$ is the PAW projector function localized within the augmentation region and obeys the relation $\langle \tilde{p}_i|\tilde{\phi}_j\rangle = \delta_{ij}$. Two projectors are constructed for each angular momentum for the ultrasoft pseudopotentials used in our calculations.

The spectra plotted correspond to a square modulus of the matrix elements,

$$I(E) = \sum_k \omega_k \sum_n \gamma(E - E_{n,k})|\langle \phi_c|r_\alpha|\psi_{n,k}\rangle|^2, \quad (2)$$

where $\gamma(E-E_{n,k})$ is a Lorentz broadening function used in Brillouin zone spectral integration. Broadening is necessary due to the limited number of sampling k points. Only transitions to unoccupied electronic states are counted. The spectra are further convolved with a Gaussian to take into account the spectral resolution. In the present work, the full width at half maximum of Lorentz and Gaussian functions are chosen to be 0.2 and 0.4 eV, respectively. For anisotropic materials (MgB_2, BeO, and β-C_3N_4), the average spectra for $\alpha = x,y,z$ were presented, which corresponds to the experimental measurement using magic angle conditions.[41]

III. RESULTS AND DISCUSSION

Generally speaking, the inclusion of the core hole can induce changes in both the shape of the spectral features and in their absolute energy position. The shift of the absolute energy comes from the deeper core-level energy due to the core electron excitation and the change in the relative energy of the final states due to the core-hole perturbation. Our focus is on the change in the spectral features induced by the core hole, and so we concentrate on the difference between ground electronic states and the "excited" electronic states. A positive core-hole potential has the effect of pulling states in the conduction band down toward the threshold energy and causing a contraction of the wave function, which will enhance the spectral weight for the spectral features near the threshold.

In order to investigate the parameters related to the strength of core-hole effects, we have carried out calculations of core excited spectra in eight different materials. The theoretical K edges for these materials with and without the inclusion of core-hole effects are shown in Figs. 1–3. The energy of the conduction band minimum is set to zero in the figures. Experimental spectra where available are also reproduced from Refs. 8, 10, 19, 38, and 42–44, shown in the figures for comparison. The experimental spectra are vertically offset for clarity. It can been seen that experimental features are well reproduced by the core-hole calculation, bearing in mind that our work concentrates on the shape of the core-level spectra and does not attempt to determine the absolute threshold energy.

For all the spectra shown in Figs. 1–3, the core-hole influence is more significant near the absorption threshold. The spatial distribution of final electronic states near the threshold is localized, with the bonding orbitals generally falling into this energy range. The transition to these final states can be heavily affected by the core hole, and this effect can extend over an energy range of up to 20 eV above the threshold. The core-hole influence for spectral features at higher excited energies is not significant. The spatial distribution of high energy excited states is extended, and their overlap with core-hole states is small, so the influence by the core-hole positive charge to the spectral features is expected to be less important.

Figure 1 shows the results for two ionic compounds LiF and BeO and a covalent compound c-BN. In the Li K edge in LiF, a prominent peak near the threshold is observed in the experimental spectrum, which is absent in the ground state spectrum but is well reproduced when the core-hole effect is included. The core-hole effect for the Be K edge in BeO is similar to that for the Li K edge in LiF; the presence of the core hole dramatically alters the distribution of spectral features; and, once again, a sharp peak near the threshold is generated. For the F K edge in LiF and O K edge in BeO, the spectral intensity has also shown significant changes compared to the ground state results within a 20 eV range above the threshold. However, the influence of the core hole is apparently less significant as compared to their cation counterparts.

In cubic boron nitride, the B-N covalent bonding has an intrinsic polar character due to the electronegativity difference between boron and nitrogen. Although core-hole effects alter the spectral features in the range 0–10 eV for both the B and N K edges, it can be seen from Fig. 1 that the difference between the ground state and the core-hole calculations for the B K edge is larger than that for the N K edge. The sharp exciton peak found in Li and Be K edges does not appear in the B K edge.

Through an examination of the theoretical K edges in Fig. 1, a qualitative conclusion can be drawn: For cations in ionic compounds or atoms with a lower electronegativity in covalent compounds, the core-level spectra are distorted by the core-hole effects to a greater extent than their counterparts with a higher electronegativity. This indicates some correla-

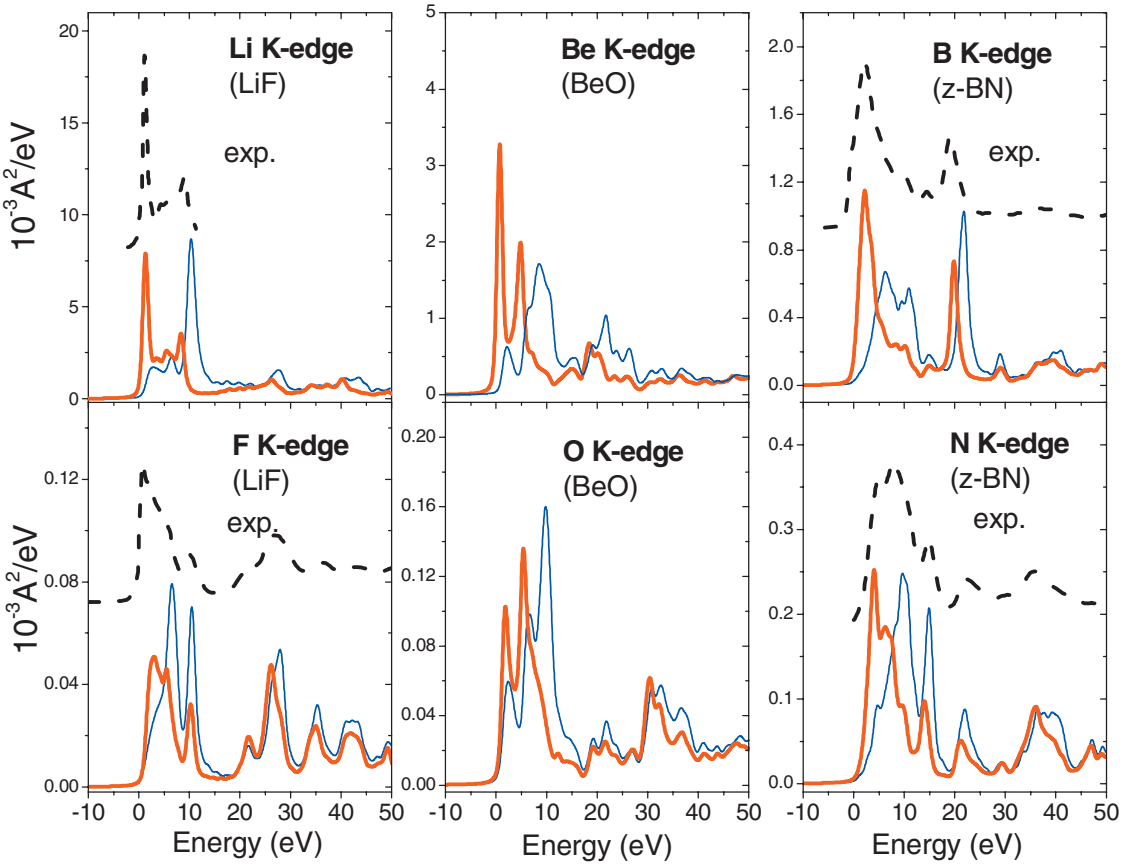

FIG. 1. (Color) Theoretical core-level excited spectra for LiF, BeO, and cubic BN with inclusion (thick red line) and without inclusion (thin blue line) of the core-hole effects. Experimental spectra (dash line) for LiF (Refs. 42 and 43) and cubic BN (Ref. 8) were reproduced from Refs. 8, 42, and 43 for comparison.

tion between the strength of core-hole effects and the valence electron screening.

Carbon K edges in β-C_3N_4, diamond, and 3C-SiC are shown in Fig. 2. In silicon carbide, carbon atoms attract valence electrons from silicon atoms, in contrast to the behavior of carbon atoms in carbon nitride. Atomic populations calculated based on a Mulliken population analysis[45] are listed in Table II. For the C K edge in β-C_3N_4, on the inclu-

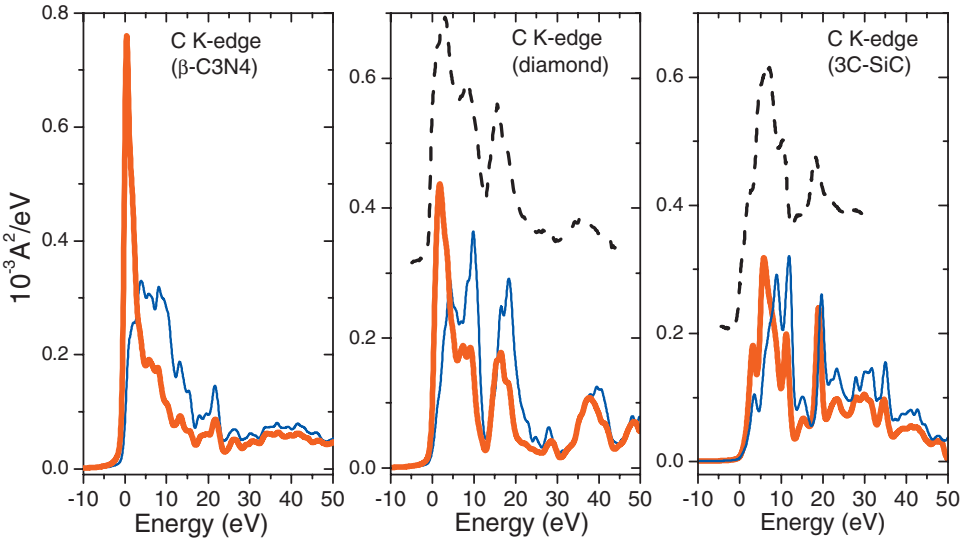

FIG. 2. (Color) Theoretical carbon K edges in β-C_3N_4, diamond, and 3C-SiC with inclusion (thick red line) and without inclusion (thin blue line) of the core-hole effects. Experimental spectra (dash line) for diamond (Ref. 10) and 3C-SiC (Ref. 44) were reproduced from references for comparison.

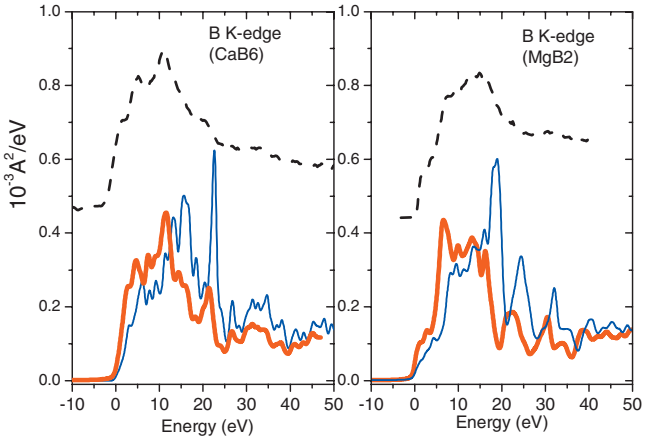

FIG. 3. (Color) Theoretical boron *K* edges in CaB_6 and MgB_2 with inclusion (thick red line) and without inclusion (thin blue line) of the core-hole effects. Experimental spectra (dash line) for CaB_6 (Ref. 38) and MgB_2 (Ref. 19) were reproduced from references for comparison.

sion of core hole a very sharp peak is formed near the threshold, but it is not present in the ground state calculation result. In contrast, the core-hole influence in the C *K* edge of 3*C*-SiC is quite weak; a one to one correspondence can be found between the spectral features with and without the inclusion of the core hole. The core-hole effect in diamond is similar, but to a lower degree as compared to the C *K* edge in β-C_3N_4.

The strength of core-hole effects in carbon *K* edges can be estimated approximately by the bonding electron transfer. The bonding electrons in cubic BN are drawn to the nitrogen atom, so the core-hole effects are quite significant in the B *K* edge (Fig. 1). This would lead us to expect that in metal borides, the core-hole effects would be relatively weak since the boron atom draws electrons from its metal counterpart. The theoretical results for CaB_6 and MgB_2 shown in Fig. 3 confirm this suggestion. The weakness of core-hole effects for the B *K* edge in MgB_2 explains previous successes in reproducing and interpreting experimental spectra using standard ground state calculations.[19,46,47]

In order to describe the core-hole influence quantitatively, the Hellinger distance is calculated to measure the spectral variation caused by the presence of the core hole, i.e., the strength of the core-hole effects. The Hellinger distance to measure the distance between two spectra, p and q, is defined as

$$D_{1/2}(p\|q) = \int_x (\sqrt{p(x)} - \sqrt{q(x)})^2 dx. \quad (3)$$

The Hellinger distance is invariant under rebinning and permutation. It is a special case (α=1/2) of α divergence,[48]

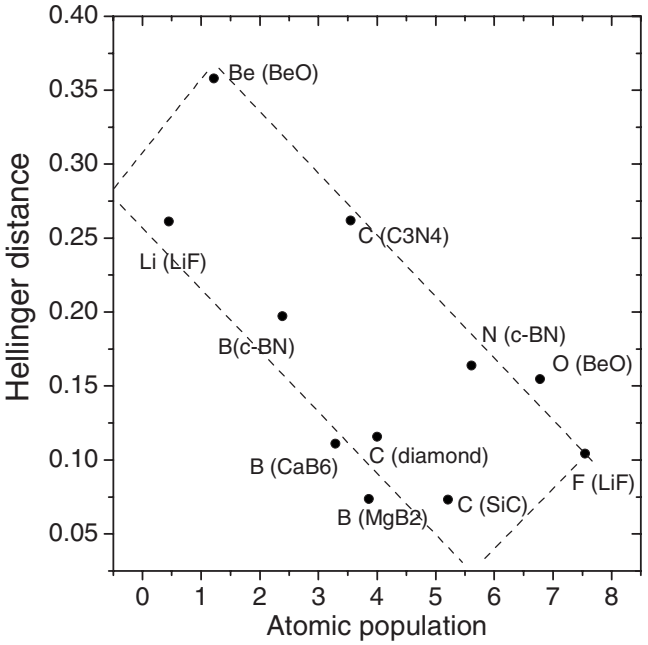

FIG. 4. Hellinger distance between calculated spectra with and without core-hole effects versus valence charge population.

which is itself a generalization of the Kullback-Leibler divergence.[49] To prepare this quantification, we shifted the ground state results with a constant energy shift so as to minimize the differences from about 15 to 45 eV, where there is less distortion due to the presence of the core hole. Then, the Hellinger distances between the ground and excited core-hole spectra in the energy window from −2 to 40 eV were calculated and normalized using the spectral intensity of excited spectra in the same range. The results are plotted in Fig. 4 against the atomic populations from the ground state calculations (Table II).

Figure 4 clearly demonstrates the relationship of valence charge population and core-hole strength. Larger differences between spectra tend to occur for smaller valence charge populations. In principle, an accurate description of the electronic relaxation in response to the core hole requires detailed information on the electronic structure. The screening effect of valence electrons is just one of the indicators, and the atomic population is itself an approximate index to rank the effect of valence electron screening. It is not surprising that the data points in Fig. 4 could not be precisely represented by trial fitting functions due to this complexity.

A connection between core-hole strength and dielectric constant has also been suggested.[20] The microscopic dielectric constant[50] might determine the core-hole strength because the core-hole effect is a reflection of microscopic dielectric response for the material system to the positive charge introduced by the core hole; however, it is different to

TABLE II. Atomic populations by Mulliken analysis.

LiF	BeO	*c*-BN	CaB_6	MgB_2	β-C_3N_4	Diamond	β-SiC
Li 0.45	Be 1.22	B 2.39	B 3.29	B 3.86	C 3.55	C 4.00	C 5.21
F 7.55	O 6.78	N 5.61					

find a well defined relation between the core-hole strength and the experimentally measured macroscopic dielectric constant. The dielectric constant for a compound has a fixed value, but the core-hole influence on different elements in the same compound is different. For example, the core-hole strength of the B *K* edge in BN is more significant than the N *K* edge. Whether a simple relation between core-hole effects and band gap or dielectric constant exists or not requires further investigation. The valence electron screening plays a crucial role in the electron-hole interaction, and our analysis has shown that it is feasible to estimate the core-hole strength of different core excitation processes by the bonding electron transfer and valence charge population connected to the excited atom.

IV. SUMMARY

A systematic study has been carried out to investigate core-hole effects in different atomic species and materials by a detailed comparison between the standard ground state calculations and more rigorous calculations that include the core-hole influence. Both qualitative observation and quantitative analysis reveal the critical role of valence electron screening in the strength of the core-hole effects. For similar compounds, core-hole effects will be more significant for core excitation spectra arising from cations in ionic compounds or from elements with lower electronegativity in covalent compounds. For a particular element in different materials, the core-hole effects will be more significant when it has a tendency to lose bonding electrons.

ACKNOWLEDGMENTS

We thank David Mackay and Daniel Corbett for helpful discussions concerning measuring the distance between two spectra. S.P.G. acknowledges the support of the Royal Society SBFT International Grant, and C.J.P. acknowledges EPSRC for funding. This research was partly funded by the National Key Research and Development Project for Basic Research from the Ministry of Science and Technology of China, and the "985" funding of Tsinghua University.

[1] S. T. Pantelides, Phys. Rev. B **11**, 2391 (1975).
[2] J. F. van Acker, W. Speier, J. C. Fuggle, and R. Zeller, Phys. Rev. B **43**, 13916 (1991).
[3] H. P. Hjalmarson, H. Buttner, and J. D. Dow, Phys. Rev. B **24**, 6010 (1981).
[4] P. Rez, J. R. Alvarez, and C. J. Pickard, Ultramicroscopy **78**, 175 (1999).
[5] S.-D. Mo and W. Y. Ching, Phys. Rev. B **62**, 7901 (2000).
[6] S. P. Gao, J. Zhu, and J. Yuan, Chem. Phys. Lett. **400**, 413 (2004).
[7] M. Taillefumier, D. Cabaret, A.-M. Flank, and F. Mauri, Phys. Rev. B **66**, 195107 (2002).
[8] D. N. Jayawardane, C. J. Pickard, L. M. Brown, and M. C. Payne, Phys. Rev. B **64**, 115107 (2001).
[9] S. Köstlmeier and C. Elsässer, Phys. Rev. B **60**, 14025 (1999).
[10] C. J. Pickard and M. C. Payne, Inst. Phys. Conf. Ser. **153**, 179 (1997).
[11] C. Hebert-Souche, P. H. Louf, P. Blaha, M. Nelheibel, J. Luitz, P. Schattschneider, K. Schwarz, and B. Jouffrey, Ultramicroscopy **83**, 9 (2000).
[12] A. J. Scott, R. Brydson, M. MacKenzie, and A. J. Craven, Phys. Rev. B **63**, 245105 (2001).
[13] J. A. Soininen and E. L. Shirley, Phys. Rev. B **64**, 165112 (2001).
[14] E. L. Shirley, Phys. Rev. Lett. **80**, 794 (1998).
[15] J. J. Rehr and A. L. Ankudinov, Int. J. Quantum Chem. **95**, 487 (2003).
[16] J. J. Rehr, J. A. Soininen, and E. L. Shirley, Phys. Scr., T **T115**, 207 (2005).
[17] A. L. Ankudinov, Y. Takimoto, and J. J. Rehr, Phys. Rev. B **71**, 165110 (2005).
[18] B. Jiang, N. Jiang, and J. C. H. Spence, J. Phys.: Condens. Matter **15**, 1299 (2003).
[19] R. Klie, H. Su, Y. Zhu, J. Davenport, J. Idrobo, N. Browning, and P. Nellist, Phys. Rev. B **67**, 144508 (2003).
[20] G. Duscher, R. Buczko, S. J. Pennycook, and S. T. Pantelides, Ultramicroscopy **86**, 355 (2001).
[21] E. L. Shirley, J. Electron Spectrosc. Relat. Phenom. **137-140**, 579 (2004).
[22] J. Zhu, S. P. Gao, A. H. Zhang, and J. Yuan, J. Electron Microsc. **54**, 293 (2005).
[23] I. Tanaka, H. Araki, M. Yoshiya, T. Mizoguchi, K. Ogasawara, and H. Adachi, Phys. Rev. B **60**, 4944 (1999).
[24] S. Nufer, T. Gemming, C. Elsasser, S. Kostlmeier, and M. Ruhle, Ultramicroscopy **86**, 339 (2001).
[25] R. Egerton, *Electron Energy Loss Spectroscopy in the Electron Microscope*, 2nd ed. (Plenum, New York, 1996).
[26] O. Stephan, M. Kociak, L. Henrard, K. Suenaga, A. Gloter, M. Tence, E. Sandre, and C. Colliex, J. Electron Spectrosc. Relat. Phenom. **114**, 209 (2001).
[27] S. Trasobares, S. P. Gao, O. Stephan, A. Gloter, C. Colliex, and J. Zhu, Chem. Phys. Lett. **352**, 7 (2002).
[28] J. Yuan and L. M. Brown, Micron **31**, 515 (2000).
[29] M. C. Payne, M. P. Teter, D. C. Allan, T. A. Arias, and D. Joannopoulos, Rev. Mod. Phys. **64**, 1045 (1992).
[30] B. Hammer, L. B. Hansen, and J. K. Norskov, Phys. Rev. B **59**, 7413 (1999).
[31] S. J. Clark, M. D. Segall, C. J. Pickard, P. J. Hasnip, M. J. Probert, K. Refson, and M. C. Payne, Z. Kristallogr. **220**, 567 (2005).
[32] D. Vanderbilt, Phys. Rev. B **41**, 7892 (1990).
[33] J. P. Perdew, K. Burke, and M. Ernzerhof, Phys. Rev. Lett. **77**, 3865 (1996).
[34] H. J. Monkhorst and J. D. Pack, Phys. Rev. B **13**, 5188 (1976).
[35] C. J. Pickard, Ph.D. thesis, University of Cambridge, 1997.
[36] A. Y. Liu and M. L. Cohen, Phys. Rev. B **41**, 10727 (1990).
[37] D. M. Teter and R. J. Hemley, Science **271**, 53 (1996).
[38] S. P. Gao, J. Jiang, M. H. Cao, J. Zhu, and J. Yuan, Phys. Rev. B **69**, 214419 (2004).

[39] S. P. Gao, A. H. Zhang, J. Zhu, and J. Yuan, Appl. Phys. Lett. **84**, 2784 (2004).
[40] P. E. Blöchl, Phys. Rev. B **50**, 17953 (1994).
[41] Y. Sun and J. Yuan, Phys. Rev. B **71**, 125109 (2005).
[42] R. Haensel, C. Kunz, and B. Sonntag, Phys. Rev. Lett. **20**, 262 (1968).
[43] E. Hudson, E. Moler, Y. Zheng, S. Kellar, P. Heimann, Z. Hussain, and D. A. Shirley, Phys. Rev. B **49**, 3701 (1994).
[44] M. Pedio, A. Giglia, N. Mahne, S. Nannarone, S. Giovannini, C. Cepek, F. Boscherini, R. Carboni, M. Benfatto, and S. Della Longa., Phys. Scr., T **T115**, 308 (2005).
[45] M. D. Segall, R. Shah, C. J. Pickard, and M. C. Payne, Phys. Rev. B **54**, 16317 (1996).
[46] Y. Zhu, A. R. Moodenbaugh, G. Schneider, J. W. Davenport, T. Vogt, Q. Li, G. Gu, D. A. Fischer, and J. Tafto, Phys. Rev. Lett. **88**, 247002 (2002).
[47] X. Kong, Y. Q. Wang, H. Li, X. F. Duan, R. C. Yu, S. C. Li, F. Y. Li, and C. Q. Jin, Appl. Phys. Lett. **80**, 778 (2002).
[48] T. Minka, Microsoft Research Technical Report No. MSR-TR-2005-173, 2005 (unpublished).
[49] S. Kullback and R. A. Leibler, Ann. Math. Stat. **22**, 79 (1951).
[50] M. S. Hybertsen and S. G. Louie, Phys. Rev. B **34**, 5390 (1986).